Hindawi Publishing Corporation
International Journal of Antennas and Propagation
Volume 2014, Article ID 690573, 10 pages
http://dx.doi.org/10.1155/2014/690573

Research Article

Interleaved-MIMO DAS for Indoor Radio Coverage: Guidelines for Planning

E. M. Vitucci,[1] F. Fuschini,[1] V. Degli-Esposti,[1] and L. Tarlazzi[2]

[1] *Dipartimento dell'Ingegneria Elettrica e dell'Informazione (DEI), Alma Mater Studiorum-Università di Bologna, 40136 Bologna, Italy*
[2] *CommScope Italy Srl, Via Mengolina 20, 48018 Faenza, Italy*

Correspondence should be addressed to E. M. Vitucci; enricomaria.vitucci@unibo.it

Received 25 May 2014; Revised 8 August 2014; Accepted 27 August 2014; Published 15 September 2014

Academic Editor: Christoph F. Mecklenbräuker

Copyright © 2014 E. M. Vitucci et al. This is an open access article distributed under the Creative Commons Attribution License, which permits unrestricted use, distribution, and reproduction in any medium, provided the original work is properly cited.

The combination of distributed antenna systems (DAS) and multiple input multiple output (MIMO) schemes opens the way to a variety of coverage solutions for indoor environment. In this paper *interleaved-MIMO (i-MIMO) DAS* indoor coverage extension strategies are studied. Their performance in high-order MIMO cases is investigated in realistic conditions through LTE-A link-level simulations, based on statistical data extracted from radio channel measurements; the impact of the deployment strategy on performance is then evaluated and useful planning guidelines are derived to determine the optimum deployment for a given propagation environment.

1. Introduction

MIMO transmission techniques are necessary for present and future indoor mobile radio systems to achieve a spectral efficiency of 30 bit/s/Hz, as required by the long term evolution-advanced (LTE-A) standard [1] or even higher figures in future-generation systems.

Differently from what happens outdoors, a large number of easily accessible fixed-terminal locations are available indoors due to the intrinsically 3-dimensional topology and to the presence of cable raceways, double ceilings, and so forth. Therefore distributed antenna systems (DAS) indoor coverage-extension schemes can be implemented where the same signal (of a single base station) is distributed to a number of remote antenna units (RAUs) using copper cables or optical fibers (F-DAS) to achieve a better radio coverage [2, 3].

The traditional MIMO implementation over a DAS scheme requires providing each RAU with all n MIMO branches signals with related cables and antenna elements: this solution may be called "colocated MIMO DAS." The upgrade from SISO DAS to "colocated MIMO DAS" can be expensive as it requires the installation of new cables and antennas elements at each RAU location and often the modification of the whole deployment.

Recent studies have shown the advantages of adopting "*distributed MIMO*" schemes where the n antenna elements relative to the n MIMO branch-signals are further spaced to exploit lower fading correlation among the different branches and therefore better performance with respect to a colocated MIMO scheme [4, 5]. Since antenna displacement can be actually realized through a DAS scheme by connecting different branches to different RAUs, such solutions are often called "MIMO DAS" and allow an easy and cheap upgrade from SISO to MIMO DAS as the antenna and cable deployment does not need to be modified at all. A drawback of this solution is represented by the uneven power distribution of different MIMO branch-signals at the *Rx* due to the different spatial placement of the corresponding antenna elements: such phenomenon is called "power imbalance" (PI), whose intensity can be, for instance, evaluated through the metrics introduced in [6].

Of course in large indoor environments with many RAU locations multiple repetitions of the n MIMO branch-signals must be deployed over the service area; the MIMO branches

must be therefore properly *interleaved* over the environment in order to simultaneously guarantee good radio coverage and low PI, therefore optimizing MIMO capacity. Such deployment strategy is called "interleaved-MIMO DAS" (i-MIMO DAS) and has been introduced and illustrated for the first time in [6, 7] with particular reference to 2 × 2 MIMO systems.

Interleaved-MIMO DAS schemes are being considered with great interest by operators and installers because they might yield a performance level comparable to that of a colocated MIMO DAS (*c*-MIMO DAS) at a much lower cost [6]. However, high PI values might degrade MIMO performance to an extent that still needs to be evaluated in relation to the DAS coverage advantages, especially for high-order MIMO schemes. As already anticipated in [6], the actual PI value distribution depends on the way the n branch antennas are interleaved in space and therefore on the i-MIMO planning strategy. Of course PI also depends on the mobile users spatial distribution, but the latter cannot be controlled and has been assumed uniform in the following study.

For these reasons, the i-MIMO DAS concept is further investigated and discussed for higher-order MIMO schemes in the present paper, where LTE-advanced link-level simulations (Section 2) together with a simple but meaningful path-loss formula are used to derive some general planning guidelines (Section 3) for high-order MIMO and for 1D (corridor), 2D, and 3D (multifloor) coverage scenarios. Such planning guidelines can be useful for the system designer to properly choose the MIMO order and i-MIMO deployment to optimize the performance to cost ratio. It is worth specifying that our study is limited to the planning of a DAS system and not of the whole mobile radio network and therefore does not consider channel allocation and interference issues.

In order to provide planning guidelines, a single benchmark system standard (LTE-advanced) has been considered and the problem has been simplified by taking into account only major parameters such as the signal-to-noise ratio (SNR) and the PI that depend on the particular i-MIMO DAS deployment. Other factors such as the multipath richness and other propagation characteristics can have an important impact on performance, but they cannot be engineered as they primarily depend on the propagation environment and therefore their role has not been deeply analyzed here. In the following we will simply assume the multipath richness to be large enough not to represent a limit to MIMO performance.

2. Interleaved-MIMO DAS Evaluation

2.1. The Concept. The application of the MIMO concept to distributed antenna systems is analyzed here with particular reference to the spatial multiplexing capability, although other transmission techniques such as *Tx* diversity are of course possible. Therefore, in the following each RAU (which carries a single "MIMO branch") is supposed to transmit a MIMO signal different from those radiated by the other RAUs belonging to the same (distributed) transmitting array. Furthermore, since each RAU defines a "cell," that is, the area where its signal strength is dominant (usually square or rectangular cells in indoor scenarios, instead of hexagonal cells, due to the shape of rooms and buildings), each cell can be therefore associated with a corresponding MIMO branch.

The present work considers the implementation of i-MIMO DAS in large indoor environments with M RAU locations (with $M \gg n$, where n is the MIMO order) where multiple repetitions of the n MIMO branch-signals are deployed over the service area. The acronym "$n \times n$ i-MIMO M-DAS" can be used to indicate an nth-order i-MIMO DAS solution with M RAUs, where each RAU is equipped with a single antenna element and the mobile terminal is equipped with an array of colocated antenna elements [6].

In case a linear layout is required and/or low-order i-MIMO schemes are considered, the best spatial deployment for the different MIMO branches can be often handled on the base of somehow evident, intuitive considerations [6].

In a 2D/3D coverage case and for high-order MIMO however the best deployment scheme may be no longer trivial, as some different, interleaved solutions might exist and should be therefore evaluated.

In order to limit the spatial PI it is intuitive that the different MIMO branches should be somehow arranged in square/rectangular "clusters" (Figure 1). Of course, different clusters can be laid over the service area in different ways; for instance, in the 8-branch case assuming a 2 by 4 cluster scheme the three solutions represented in Figure 1 can be considered: the clusters can be simply aligned to each other (Figure 1—left) or a 1-/2-cell shift can be introduced between adjacent columns (or rows) of clusters (Figure 1 center and right, resp.).

Intuitively, the 2-shift solution should lead to a more uniform branch-signal distribution; however, actual performance must be assessed by simulation as shown in Section 3.

In conclusion, irrespective of the i-MIMO order, the concept of "*cluster*," widely used in cellular radio planning, applies here. However, here the mechanisms are somewhat reversed as in traditional cellular planning the cluster-size should be *large enough* to separate cochannel cells and thereby minimize interference and in i-MIMO DAS the cluster dimension and therefore the MIMO order n should be small enough to minimize power imbalance. In fact high-order MIMO deployments (such as the 8-branch case of Figure 1) will necessarily yield greater spatial spreading of branches and therefore higher PI, especially in propagation environments where path-loss increases rapidly with distance. Further i-MIMO DAS planning considerations will be provided in Section 3.

2.2. Measurement Data Overview. In order to effectively set up the system level simulations described in the next subsection some major parameters of the i-MIMO DAS channel have been preliminarily investigated through an extensive measurement campaign carried out in a typical modern indoor office, where up to 4 RAUs have been considered and several measurement routes have been deployed in different rooms and along a corridor. All measurements have been performed in static conditions at the frequency of 858 MHz for a 2 × 2 i-MIMO arrangement. In order to get rid of the local multipath effects, the measured data have been

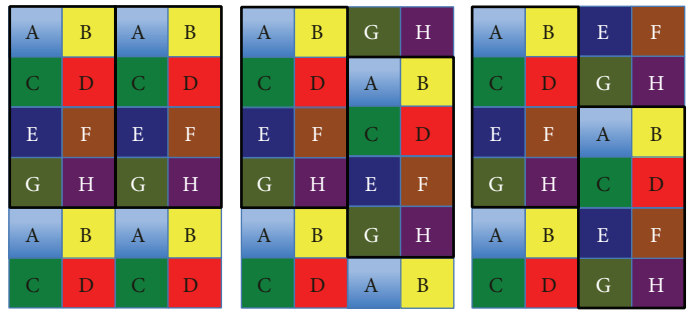

Figure 1: Uniform, 2D 8 × 8 i-MIMO DAS coverage. Left: no-shift interleaved coverage solution. Center: 1-shift interleaved coverage solution. Right: 2-shift interleaved coverage solution. The 2 by 4 branch "cluster" is highlighted in black. Each color/letter corresponds to a different MIMO branch-signal.

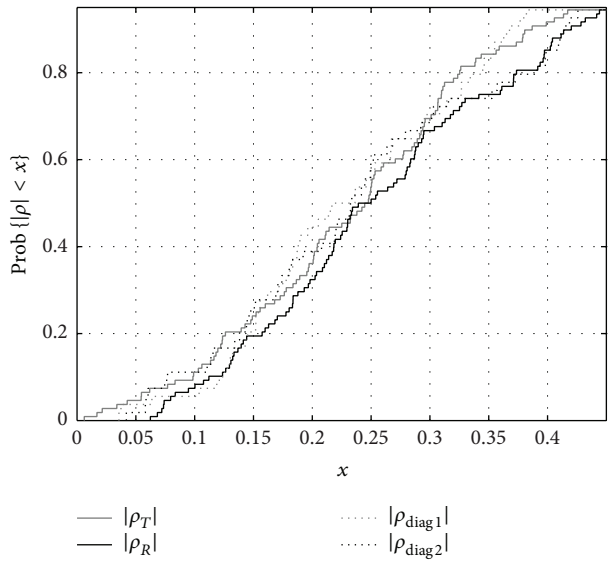

Figure 2: CDF of the magnitude of the correlation coefficients extracted from the measurements.

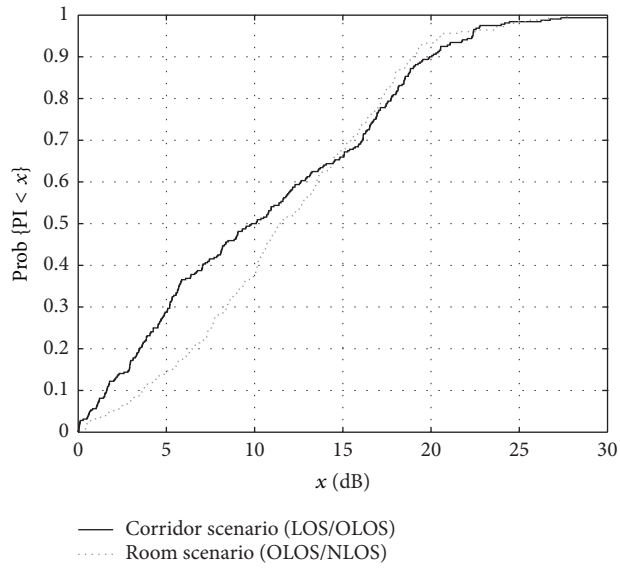

Figure 3: Experimental CDF of the PI in the considered scenarios.

collected several times moving the receiving array over a spatial grid centered on each measurement position. Further details about the measurement campaign can be found in [6, 7].

The overall amount of gathered experimental data has been postprocessed to achieve the statistics of both the channel correlations and the power imbalance. In particular, Figure 2 shows the cumulative distribution function (CDF) of the magnitude of the complex correlation coefficients (i.e., the normalized complex covariances between the elements of the channel matrix). The correlation coefficients at the transmitter/receiver side and the diagonal correlations have been computed according to the following expressions:

$$\rho_{T,i} = \left.\frac{\operatorname{cov}\left(h_{i1}, h_{i2}^{*}\right)}{\sqrt{\operatorname{cov}\left(h_{i1}, h_{i1}^{*}\right)\operatorname{cov}\left(h_{i2}, h_{i2}^{*}\right)}}\right|_{i=1,2},$$

$$\rho_{R,j} = \left.\frac{\operatorname{cov}\left(h_{1j}, h_{2j}^{*}\right)}{\sqrt{\operatorname{cov}\left(h_{1j}, h_{1j}^{*}\right)\operatorname{cov}\left(h_{2j}, h_{2j}^{*}\right)}}\right|_{j=1,2},$$

$$\rho_{\text{Diag1}} = \frac{\operatorname{cov}\left(h_{11}, h_{22}^{*}\right)}{\sqrt{\operatorname{cov}\left(h_{11}, h_{11}^{*}\right)\operatorname{cov}\left(h_{22}, h_{22}^{*}\right)}},$$

$$\rho_{\text{Diag2}} = \frac{\operatorname{cov}\left(h_{12}, h_{21}^{*}\right)}{\sqrt{\operatorname{cov}\left(h_{12}, h_{12}^{*}\right)\operatorname{cov}\left(h_{21}, h_{21}^{*}\right)}}. \quad (1)$$

All the CDFs appear rather similar, with median values always between 0.2 and 0.25 and correlation values seldom larger than 0.4. Such results clearly support the assumption—made at the end of the introduction—that multipath richness should not represent a limit to the performance of an i-MIMO system, which is therefore mainly affected by path-loss and shadowing, which practically determine the value of both the PI and the SNR.

The experimental CDF of the power imbalance is shown in Figure 3 for two different scenarios: in the "corridor" case propagation occurred in line of sight (LOS) or obstructed-LOS (OLOS) conditions (depending on the RAUs position), whereas OLOS or non-LOS conditions have been observed in the "room" case [6]. The PI values have been computed according to the expression introduced in [6] for a 2 × 2

MIMO system. The PI values range from 0 to 30 dB with a median value equal to about 10 dB in both cases, though a slightly larger value spread can be noticed in the "corridor scenario" as the CDF is less steep around the median value.

As described in the next subsection, in order to effectively assess the performance of i-MIMO DAS systems, the statistics shown in Figures 2 and 3 are used to generate realistic random channel realizations to be input into the LTE-A link-level simulator. A more detailed analysis of the MIMO channel characteristics in the considered environment can be found in [6].

2.3. Performance Evaluation of High-Order i-MIMO DAS. A wireless system must be able to cope with high downlink PI in order to achieve good performance in i-MIMO DAS configuration. For MIMO systems of order higher than 2×2, a unique PI value cannot be defined, since different branch pairs can undergo different imbalance values. Therefore, in order to estimate the average imbalance level experienced on a single *Rx* (mobile) location, the following standard deviation parameter can be adopted [6]:

$$\sigma_P = \sqrt{\frac{1}{n}\sum_{i=1}^{n}\left(P_i - \mu_P\right)^2} \quad \text{where } \mu_P = \frac{1}{n}\sum_{i=1}^{n} P_i, \tag{2}$$

where P_i is the total power (in dB units) received from all the RAUs radiating the same ith MIMO branch-signal. P_i is of course the local average of the received signal power from the ith *Tx* branch, made over all *Rx* antenna elements. Clearly, the parameter σ_P represents the standard deviation of the values $\{P_1, P_2, \ldots, P_n\}$, whereas μ_P is the average received power from all the n *Tx* MIMO branches. Assuming a constant noise power level N_0 for all the MIMO branches, the σ_P parameter can also be expressed as

$$\sigma_P = \sqrt{\frac{1}{n}\sum_{i=1}^{n}\left(\mathrm{SNR}_i - \overline{\mathrm{SNR}}\right)^2}, \tag{3}$$

where $\mathrm{SNR}_i = P_i(\mathrm{dBm}) - N_0(\mathrm{dBm})$ and $\overline{\mathrm{SNR}} = \mu_P(\mathrm{dBm}) - N_0(\mathrm{dBm})$ are the signal-to-noise ratio for the ith branch and the signal-to-noise ratio averaged over all the branches, respectively.

As a benchmark to study i-MIMO performance and planning strategies in real-life cases, the LTE-advanced standard is considered in the present work [1]. An LTE-A link-level simulator developed at Vienna University of Technology [8] is run in single-user MIMO mode, in the 2×2, 4×4, and 8×8 MIMO cases, adopting standard ITU-R power-delay profiles (PDPs) for indoor environment (indoor office channel A) [9]. Every simulation run consists of $15 \times 100 = 1500$ snapshots corresponding to 15 different SNR values from 0 to 70 dB and 100 MIMO channel matrix realizations for each SNR value.

For each realization, the channel matrices have been randomly generated according to the full-correlation model (see [10, page 72]): $\mathbf{H} = \mathbf{R}^{1/2}\mathbf{H}_w$, where $\mathbf{R}$ is the $n^2 \times n^2$ full-correlation matrix [10] whose elements are randomly generated according to the statistics shown in Figure 2, and $\mathbf{H}_w$ is a random iid channel matrix.

Then, random imbalances between the MIMO branches have been also introduced, according to the PI statistics shown in Figure 3. In particular, for each realization, random power imbalances varying between 0 and 30 dB are introduced between the columns of the channel matrix, by taking the first column as a reference and properly scaling the others. Finally, the generated MIMO channel matrices have been normalized with respect to the expectation of the square root of the average power gain of each channel realization, according to

$$\widehat{\mathbf{H}} = \frac{\mathbf{H}}{\beta} \quad \text{with } \beta = E\left[\sqrt{\frac{\sum_{i,j}\left|h_{ij}\right|^2}{n^2}}\right] = \frac{E\left[\|\mathbf{H}\|_F\right]}{n}, \tag{4}$$

where $\|\mathbf{H}\|_F$ is the Frobenius norm of the channel matrix (see also [10, page 74]), $\widehat{\mathbf{H}}$ is the normalized channel matrix, and n is the MIMO order. The main input data of the LTE-A simulator are the normalized channel matrices and the average signal-to-noise ratio $\overline{\mathrm{SNR}}$. Other simulator parameter settings are the same as in [6, 11].

The final outcome of the simulations is the downlink channel-throughput as a function of σ_P and of the average signal-to-noise ratio, as shown in Figures 4 and 5.

Figures 4 and 5 depict the simulated throughput results obtained for the 2×2 and 8×8 i-MIMO cases, respectively. A similar result has been found for the 4-branch arrangement, not represented here for the sake of brevity.

It is worth noticing that the throughput plot versus SNR and σ_p for the 2×2 case ($n = 2$) in Figure 4 is very similar to the corresponding one shown in [6], where the channel matrices given in input to the LTE simulator have been computed through ray tracing simulations [12] in a specific, representative indoor environment and not randomly generated on the base of some preassigned statistical distributions; the satisfactory agreement supports the effectiveness of the general approach here adopted, not aiming at investigating single, specific cases but rather at identifying some general but meaningful planning rules.

The results for high-order i-MIMO DAS arrangements provide manifold confirmations of the outcomes of the analysis already carried out in [6] in the 2×2 MIMO case:

(i) different "throughput zones," that is, portions of the (SNR, σ_P) plane associated with approximately the same throughput value, are clearly highlighted;

(ii) the throughput values seem to increase with SNR and on the contrary decrease for increasing power imbalance;

(iii) the full-throughput achievable within the 8×8 case ($\approx$600 Mbps) is 4 times the one achievable in the 2×2 case ($\approx$150 Mbps), as it should be according to the known theory that MIMO capacity is proportional to MIMO order if multipath is sufficiently rich;

(iv) since the simulated throughput values corresponding to different channel realizations having the same σ_P are very similar, σ_P together with the SNR can be considered a reliable performance-determining parameter.

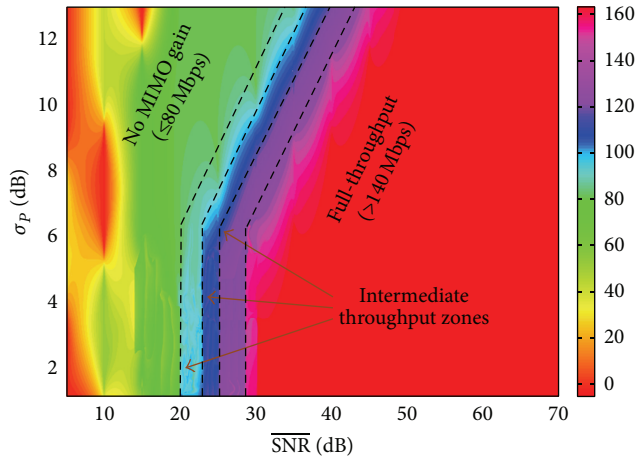

Figure 4: Downlink throughput values provided by the LTE-A link-level simulator for the 2 × 2 i-MIMO case as a function of average SNR and σ_P.

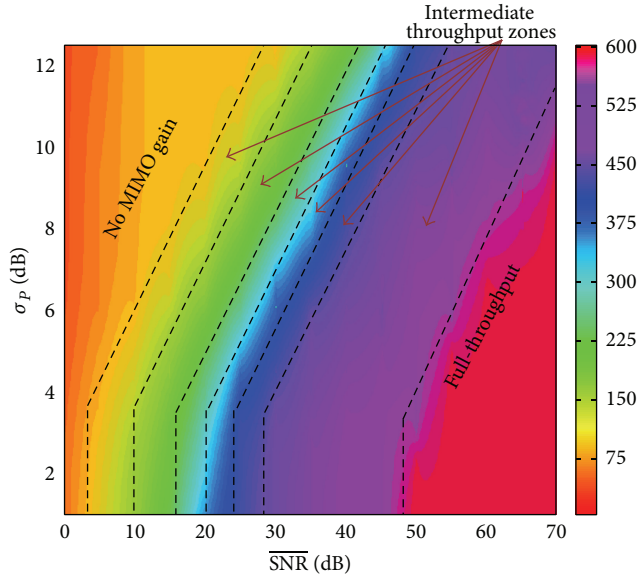

Figure 5: Downlink throughput values provided by the LTE-A link-level simulator for the 8 × 8 i-MIMO case as a function of average SNR and σ_P.

With regard to the planning guidelines of Section 3 it should be highlighted that both σ_P and SNR have been defined as "incoherent," large-scale parameters; that is, their values are independent of the phase relations between the signals at the *Rx* antennas. i-MIMO DAS system planning can be therefore based on path-loss and shadowing (obstructions) considerations only, neglecting small-scale fading effects. The throughput plots shown above, and in particular the information regarding the throughput zones, are then used in the present work in combination with a proper path-loss formula to map performance for different i-MIMO DAS deployments, as shown in the following section.

It is worth noticing that also multiuser MIMO is included in the LTE-A standard where different branches in an i-MIMO scheme would be used to serve different users. Although the i-MIMO concept and the methodological approach of this work are still valid, the PI and thus the σ_p will play a different role in that case. In fact interuser interference minimization considerations might suggest pursuing high PI values, which is the opposite of what should be pursued in single-user cases.

3. Planning Considerations

In this section, considerations and guidelines for the planning and the deployment of i-MIMO DAS systems in reference, regular 1D (corridor), 2D (single floor), and 3D (multifloor) layouts are provided on the base of both the throughput plots of Section 2.2 and the following path-loss formula, introduced and parameterized in [13]:

$$\text{PL}_{\text{dB}}(d) = \text{PL}(d_0) + 10 \cdot \alpha \cdot \log\left(\frac{d}{d_0}\right) + \beta \cdot d, \qquad (5)$$

where α is the path-loss exponent mainly accounting for the wavefront divergence and β is the specific-attenuation accounting for obstructions. Equation (5) has been shown to well reproduce path-loss as a function of link distance, compared to measurements in reference indoor environments.

In [13] it was also shown that the values of the specific-attenuation lie between 0.5 and 1.5 in most indoor office scenarios, depending on the electromagnetic characteristics and thickness of the walls, while the most appropriate value for alpha is equal to 2, with the exception of large indoor scenarios, such as shopping malls or airports. For this reason, in the following we will assume $\alpha = 2$ and $0 \leq \beta \leq 1.5$ ($\beta = 0.5$ is the reference value for the measurement scenario described in Section 2.2, as shown in [13]).

Given a propagation environment, that is, specific-attenuation β in (5), throughput performance mainly depends on PI (σ_P) and SNR, as shown in Section 2.2. Therefore i-MIMO DAS planning can be based on a two-step procedure.

(1) *SNR-Based Planning*. RAU antenna spacing and Tx power should be chosen so as to guarantee a sufficiently high SNR all over the service area and in particular at cell border.

(2) *PI-Based Planning*. The different MIMO branch-signals should be distributed over the RAU antennas in a proper "interleaved" fashion to minimize σ_P, as shown in Section 2.2. In addition, since high-order i-MIMO DAS deployments and/or high β values in (5) lead to high PI between the different branch-signals, then MIMO order should be matched to the propagation characteristics in order for σ_P to remain low enough. In other words, an increase in the MIMO order could yield a less-than-proportional increase in throughput if PL increases too rapidly with distance so as to produce a too-high power imbalance.

There is therefore affinity between i-MIMO DAS planning and traditional cellular planning, where radio coverage must be provided in the first step and then the cluster-size must be chosen so as to satisfy signal-to-interference (SIR) requirements. Here the MIMO order n plays a similar role as cluster-size while PI replaces SIR.

Since planning step (1) does not depend on the planning strategy and higher attenuation conditions or greater RAU spacing can be easily compensated with a proportional Tx power increase, step (1) will not be addressed in the following. A typical RAU antenna spacing of 20 m will be considered, whereas realistic Tx power and β values will be assumed from case to case.

On the contrary, planning step (2) will be investigated in some detail. In particular, (5) can easily provide the SNR and the σ_P values for every possible position of the receiver on the service area; then, the corresponding system performance can be evaluated by means of the throughput plots obtained with the LTE-A simulator, that is, by identifying the corresponding throughput zone for each pair (SNR, σ_P).

It is worth noticing that hereafter the performance of the i-MIMO solutions will not be evaluated in terms of absolute throughput, but rather in terms of "average (relative) gain with respect to the SISO case" (n_G), which is of course defined as the ratio between the actual system throughput (evaluated through the previously described procedure) and the SISO maximum throughput:

$$n_G = \frac{\text{Average MIMO throughput}}{\text{Max SISO throughput}} \quad (0 \leq n_G \leq n). \tag{6}$$

According to this definition, n_G ranges from 0 to n, n being the MIMO order (2, 4, or 8 have been here considered). The n_G value can be interpreted as the "equivalent" number of branches which contribute to achieving the full MIMO capacity gain (useful branches). For instance, if n_G is equal to n, it means that all branches are successfully exploited and therefore the full MIMO throughput is achieved. In the following text, $\overline{n_G} \stackrel{\text{def}}{=} n - n_G$ instead of n_G is often used, since the corresponding plots usually appear more readable: $\overline{n_G}$ can be interpreted as the number of branches "under-threshold" which do not contribute to the MIMO capacity gain.

In general, if $n_G \ll n$ (or, equivalently, $\overline{n_G} \gg 0$), then the considered interleaved solution is seriously ineffective. This is due to the above-mentioned problem: when the MIMO order n is overdimensioned, then the i-MIMO "cluster" is too big and power imbalance is too high to effectively exploit all MIMO branches.

It is therefore very important to choose the appropriate MIMO order n for the considered propagation environment to avoid unprofitable efforts (high-order systems are much more complex and expensive than low-order systems) for no or little performance gain.

If $n_G \ll n$ adequate countermeasures should be adopted, such as a different distribution of the MIMO branches in the space, an increase of the transmitted RAU power, or, if the above-mentioned parameters are already optimized, a reduction of the MIMO order.

In summary the present section provides the following useful results:

(i) different i-MIMO DAS deployment solutions are evaluated to identify the best one, especially in 2D and 3D cases where different, apparently equivalent solutions are possible, as highlighted in Section 2.1;

(ii) for each reference case, the equivalent number of useful branches is determined as a function of RAU Tx power and specific-attenuation β: this is a very important result to optimize planning and avoid waste of power or MIMO order overdimensioning.

Three reference, regular 1D (corridor), 2D (single floor), and 3D (multifloor), layouts are considered in Sections 3.1, 3.2, and 3.3, respectively. In all cases the considered service area, that is, the target area where mobile terminals are located, is assumed separated in space (1.5 m apart along a vertical axis) from the plane where RAUs are located (e.g., the ceiling) to avoid power singularities. This means that the mobile terminal is always at a distance of at least 1.5 m away from the closest RAU antenna. A uniform mobile user distribution is assumed in all cases.

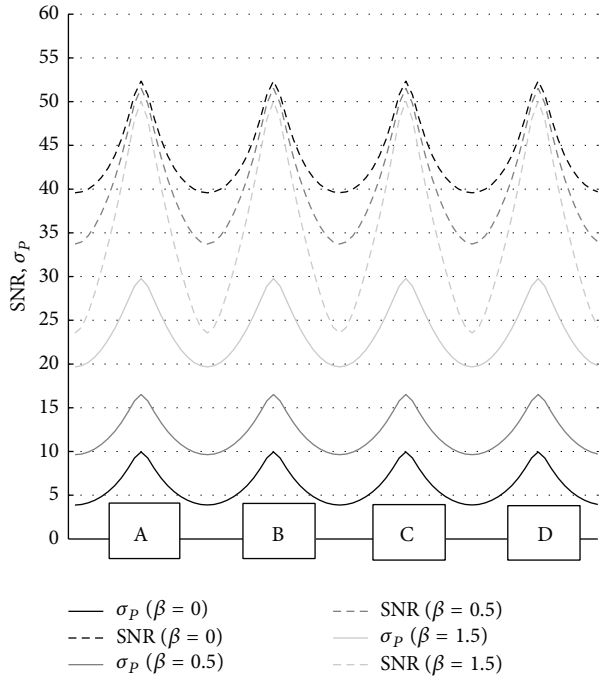

Figure 6: Behaviour of σ_P and SNR in a 4-branch i-MIMO linear deployment for different values of the propagation model parameters (RAU antenna distance: 20 m).

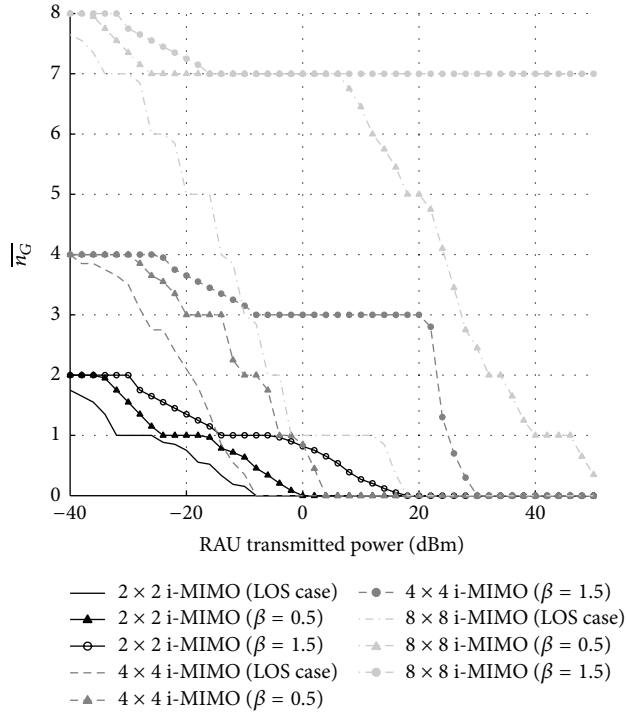

Figure 7: Comparison of 2-, 4-, and 8-branch i-MIMO DAS performance in the linear deployment (corridor) case. Average number of branches under threshold ($\overline{n_G}$) is shown for different values of the propagation model parameters (RAU antenna distance: 20 m).

3.1. Linear Deployment (RAUs Placed along a Corridor). If a linear deployment is considered (e.g., RAUs positioned along a corridor) and assuming that the receiver moves along a route parallel to the corridor where the RAUs are located, both SNR and σ_P values peak in proximity to each RAU and on the contrary reach their minimum close to the middle point between adjacent RAUs.

This behavior is clearly confirmed by the example in Figure 6, which refers to a 4-branch arrangement for different β values (β = 0 of course corresponds to an ideal LOS condition).

It is evident that the better the SNR, the worse the PI and vice versa; therefore, the system design (i.e., the RAUs' spatial deployment and the choice of the MIMO order) should aim at properly balancing coverage (SNR) and imbalance (σ_P) over the service area.

Figure 7 represents $\overline{n_G} = n - n_G$ as a function of the power transmitted by each RAU antenna for different MIMO orders and different values of the propagation parameter.

It is worth noticing that the larger the MIMO order, the higher the performance sensitivity to the propagation conditions. In fact, $\overline{n_G}$ seems to be weakly dependent on β in the 2 × 2 case, whereas performance is dramatically different for different β values in the 8 × 8 case.

Low $\overline{n_G}$ values in Figure 7 should be pursued when planning a linear i-MIMO DAS system. In practice, the 2-branch case seems to be almost always a feasible solution, whereas the adoption of the 4-branch deployment could be questionable with β = 1.5 since a quite high power level (at least 25 dBm) would be required to achieve a good

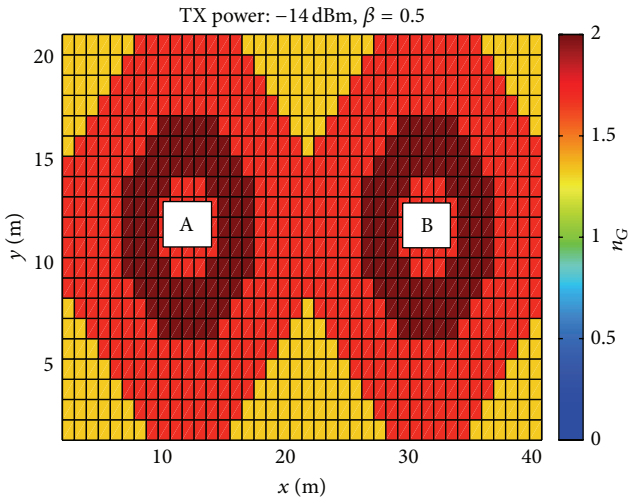

Figure 8: Performance of 2 × 2 i-MIMO DAS in a 2D deployment case. Relative gain with respect to SISO is shown (RAU antenna power: −14 dBm; β = 0.5; RAU antenna distance: 20 m).

performance. For the same reason the 8-branch solution is clearly unfit except for the LOS case.

3.2. 2D Deployments. The combined effects of SNR and σ_p on the performance of an i-MIMO DAS system are further explained in Figures 8 and 9, which represent two examples

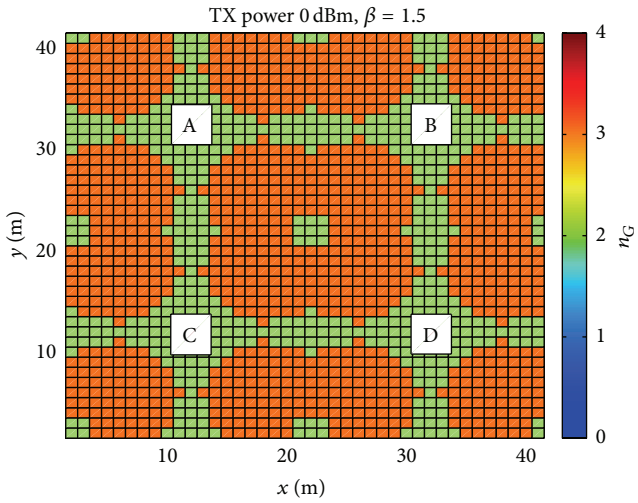

FIGURE 9: Performance of 4 × 4 i-MIMO DAS in a 2D deployment case. Relative gain with respect to SISO is shown (RAU antenna power: 0 dBm; β = 1.5; RAU antenna distance: 20 m).

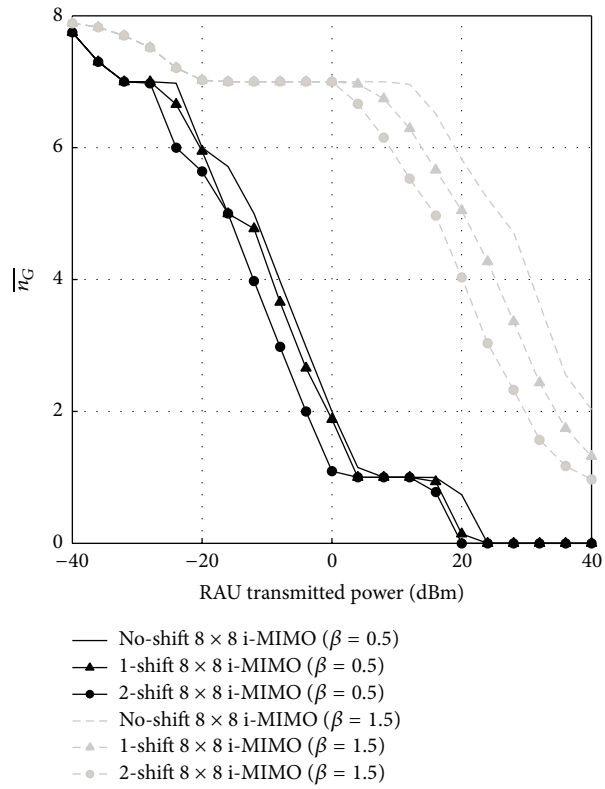

FIGURE 10: Performance comparison of different 8-branch i-MIMO 2D deployments (no-shift, 1-shift, and 2-shift). Average number of branches under threshold ($\overline{n_G}$) is shown, for different values of the propagation model parameters (RAU antenna distance: 20 m).

of 2D spatial distribution of the n_G values over the cluster area in the 2- and the 4-branch arrangement, respectively.

In both cases, the best performance (i.e., the highest n_G values) is achieved not too close to the RAUs, where the high imbalance prevails over the large SNR values, or too far from them, where the received signal (and therefore the SNR) is weak.

Two different values of β are considered in Figures 8 and 9 to better highlight the different performance zones.

The effectiveness of the interleaved approach is evaluated in Figure 10 for different shift value. The analysis is limited to the 8-branch arrangement since only a negligible difference has been appreciated between the shift and the no-shift solutions in the 4-branch case.

The benefit provided by a shifted deployment is slight if β = 0.5, whereas it becomes more evident for β = 1.5; a plausible reason is that in presence of more favorable propagation conditions (β = 0.5) the power imbalance is likely under control (on the average) even without any shift; on the contrary, worse propagation conditions (β = 1.5) produce an increase of the imbalance, which can be then partly reduced introducing the shift, which restores a more uniform branch-power spatial distribution.

A performance comparison for different MIMO order values is presented in Figures 11 and 12 in terms of $\overline{n_G}$ and percentage of area where users achieve "good throughput," that is, a throughput greater than 75% of the maximum achievable given the MIMO order.

Similarly to the 1D case, Figure 11 highlights the fact that a MIMO solution with order 2 can easily provide satisfactory performance irrespective of the propagation condition in the 2D case. On the contrary, the theoretical potential of the 8-branch arrangement cannot be fully exploited in hostile propagation environment: if β = 1.5 and assuming 25 dBm as the upper limit for the RAU transmitted power, then n_G cannot exceed 5.

The 4-branch case represents an intermediate case, but more specifically it shows a more marked similarity to the 2-branch solution, since the RAU transmitted power required to reach the full MIMO throughput ($\overline{n_G}$ = 0) is almost the same for the two deployments (Figure 11). This is also confirmed in Figure 12, where the curves related to the 2- and 4-branch cases are nearly overlapped. From Figure 12 the minimum Tx power to achieve good performance can be inferred in the different cases. For example, in a 4×4 case with β = 1.5, a Tx power of at least a couple of dBm is necessary to achieve "good throughput" (i.e., a throughput greater than 75% of the maximum) over 90% of the coverage area.

3.3. 3D Deployments (Outline). For the sake of brevity, the analyses of the 3D case are here limited to the solution represented in Figure 13, where a 4th order i-MIMO DAS system is deployed over 3 different floors.

The 2 × 2 square cluster is repeated over each floor according to the no-shift coverage solution shown in Figure 3 (center), whereas a possible "diagonal shift" (i.e., achieved through two subsequent shifts in the x- and in the y-direction, resp.) is considered between adjacent floors.

Moreover, an additional floor penetration loss of 10 dB is considered for the evaluation of the intensity of the signals received from RAUs placed on different floors with respect to the receiver.

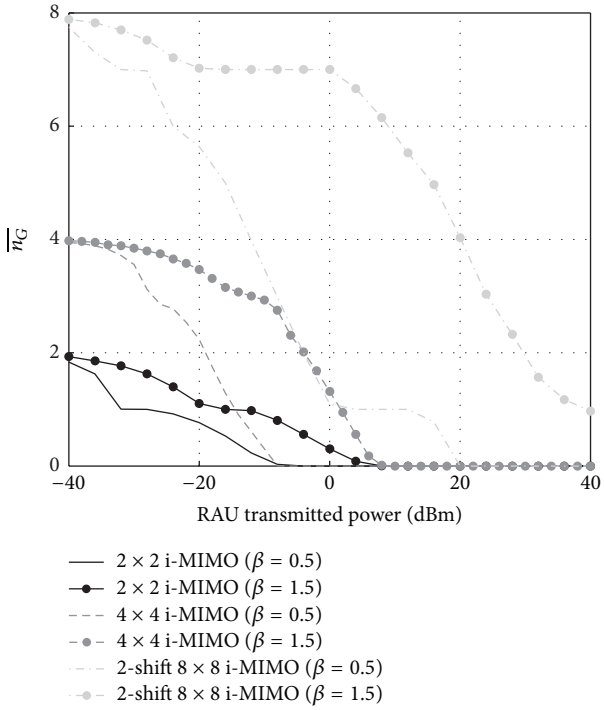

Figure 11: Comparison of 2-, 4-, 8-branch i-MIMO DAS average performance in the 2D deployment case. Average number of branches under threshold ($\overline{n_G}$) is shown, for different values of the propagation model parameters (RAU antenna distance: 20 m).

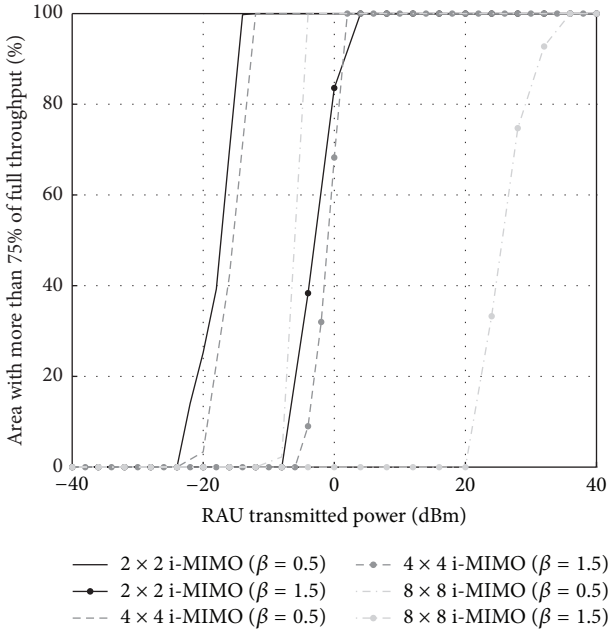

Figure 12: Comparison of 2-, 4-, and 8-branch i-MIMO DAS performance (% of area where more than 75% of maximum throughput is achieved) in the 2D deployment case, for different values of the propagation model parameters (RAU antenna distance: 20 m).

System performance is represented in Figure 14 and clearly shows that no significant performance improvement is provided by the shifted solution for $\beta = 0.5$. In this case the achieved result is essentially the same as in the 2D case (Figure 11): propagation over the same floor is dominant with respect to "interfloor" propagation.

On the contrary, if $\beta = 1.5$ "intrafloor" propagation becomes more difficult and therefore signals coming from different floors are no longer negligible. According to Figure 14, the shift solution yields in this case better performance, as it provides—on the average—a lower power imbalance.

4. Conclusion

Planning strategies for interleaved-MIMO DAS indoor coverage-extension solutions are studied in the present paper. Although LTE-A standard is adopted as a benchmark here, the proposed methodology, which is based on large-scale propagation parameters such as SNR and power imbalance (PI, measured through σ_P) and on a simple path-loss formula, is valid also for interleaved-MIMO DAS solutions implemented on different systems.

Results show that proper, interleaved deployment solutions based on the concept of "cluster" should be adopted to keep PI low enough. In some 2D and 3D deployment cases a cluster-shifting can help further performance optimization.

PI is shown to increase with both MIMO order n and specific-attenuation β and to decrease with coverage-layout

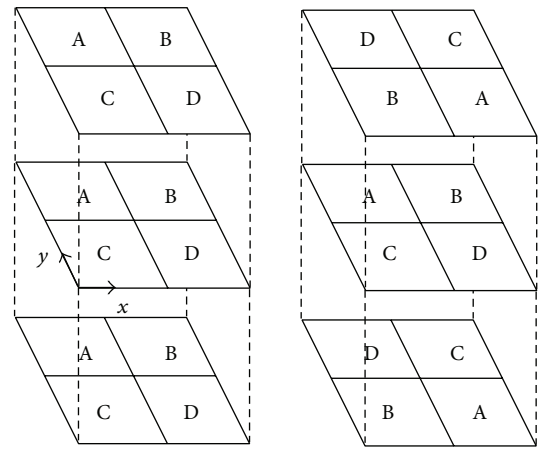

Figure 13: 3D 4 × 4 i-MIMO DAS coverage. Left: noninterleaved coverage solution. Right: coverage solution with branch interleaving between different floors.

dimensions, as 2D or 3D solutions allow a more uniform *hearability* of a larger number of MIMO branches at the generic *Rx* position than 1D solutions.

It is wrong to adopt, say, a costly 8 × 8 i-MIMO DAS solution in a 1D-deployment with a large specific-attenuation as most MIMO branches would be useless and full-throughput could never be achieved.

Therefore, useful planning guidelines are proposed and graphs are derived to help the i-MIMO system designer determine the maximum MIMO order for which performance is not yet limited by power imbalance and therefore the best i-MIMO solution for given traffic and propagation conditions.

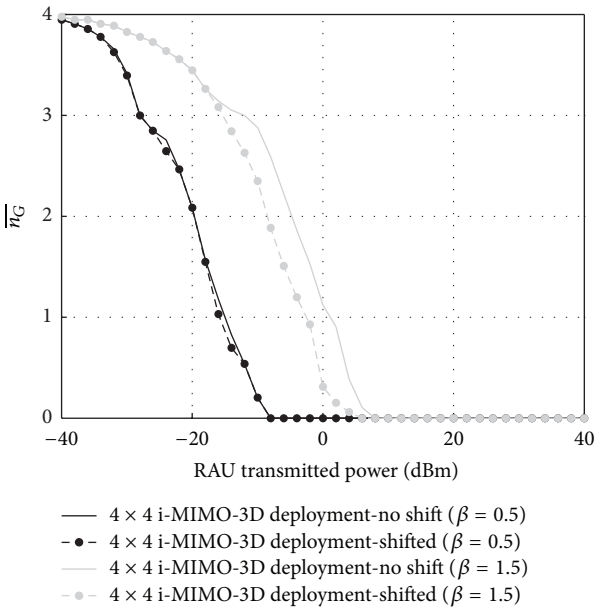

Figure 14: Performance comparison of 4 × 4 i-MIMO no-shift and diagonal-shifted 3D deployments. Average number of branches under threshold ($\overline{n_G}$) is shown (RAU antenna horizontal distance: 20 m; RAU antenna vertical distance: 3 m; floor attenuation factor: 10 dB).

Conflict of Interests

The authors declare that there is no conflict of interests regarding the publication of this paper.

Acknowledgments

This work has been carried out in the framework of and partly funded by the EU Project Architectures for Flexible Photonic Home and Access Networks (ALPHA), ICT CP-IP 212 352. This work has also been partly funded by the European Network of Excellence NEWCOM++. The authors thank their graduate student Stefano Fiaschi for the great help in carrying out system simulations.

References

[1] IEEE 3GPP TS 36.211 V11.1.0, "Physical channels and modulation (Release 11)," 2012.

[2] A. A. M. Saleh, A. J. Rustako Jr., and R. S. Roman, "Distribute Antennas for Indoor Radio Communications," *IEEE Transactions on Communications*, vol. 35, no. 12, pp. 1245–1251, 1988.

[3] M. Fabbri and P. Faccin, "Radio over fiber technologies and systems: new opportunities," in *Proceeding of the 9th International Conference on Transparent Optical Networks (ICTON '07)*, pp. 230–233, Rome, Italy, July 2007.

[4] R. Ibernon-Fernandez, J.-M. Molina-Garcia-Pardo, and L. Juan-Llacer, "Comparison between measurements and simulations of conventional and distributed MIMO system," *IEEE Antennas and Wireless Propagation Letters*, vol. 7, pp. 546–549, 2008.

[5] M. Alatossava, A. Taparugssanagorn, V.-M. Holappa, and J. Ylitalo, "Measurement based capacity of distributed MIMO antenna system in Urban microcellular environment at 5.25 GHz," in *Proceedings of the IEEE 67th Vehicular Technology Conference-Spring (VTC '08)*, pp. 430–434, May 2008.

[6] E. M. Vitucci, L. Tarlazzi, F. Fuschini, P. Faccin, and V. Degli-Esposti, "Interleaved-MIMO DAS for Indoor radio coverage: concept and performance assessment," *IEEE Transactions on Antennas and Propagation*, vol. 62, no. 6, pp. 3299–3309, 2014.

[7] L. Tarlazzi, P. Faccin, E. M. Vitucci, F. Fuschini, and V. Degli-Esposti, "Characterization of an interleaved F-DAS MIMO indoor propagation channel," in *Proceedings of the 6th Loughborough Antennas and Propagation Conference (LAPC '10)*, pp. 505–508, Loughborough, UK, November 2010.

[8] C. Mehlführer, M. Wrulich, J. C. Ikuno, D. Bosanska, and M. Rupp, "Simulating the long term evolution physical layer," in *Proceedings of the 17th European Signal Processing Conference (EUSIPCO '09)*, Glasgow, UK, 2009.

[9] ITU-R Recommendation M.1225, "Guidelines for evaluation of radio transmission technologies for IMT-2000," 1997.

[10] B. Clerckx and C. Oestges, *MIMO Wireless Networks*, Academic Press (Elsevier), Oxford, UK, 2nd edition, 2013.

[11] E. M. Vitucci, L. Tarlazzi, P. Faccin, and V. Degli-Esposti, "Analysis of the performance of LTE systems in an Interleaved F-DAS MIMO indoor environment," in *Proceedings of the 5th European Conference on Antennas and Propagation (EuCAP '07)*, pp. 2184–2186, Rome, Italy, April 2007.

[12] E. M. Vitucci, V. Degli-Esposti, and F. Fuschini, "MIMO channel characterization through ray tracing simulation," in *Proceedings of the 1st European Conference on Antennas and Propagation (EuCAP '06)*, Nice, France, November 2006.

[13] V. Degli-Esposti, G. Falciasecca, F. Fuschini, and E. M. Vitucci, "A meaningful indoor path-loss formula," *IEEE Antennas and Wireless Propagation Letters*, vol. 12, pp. 872–875, 2013.

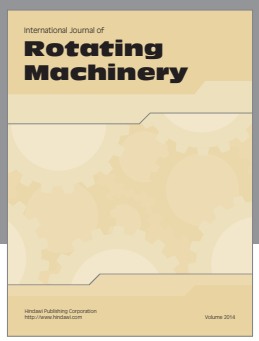

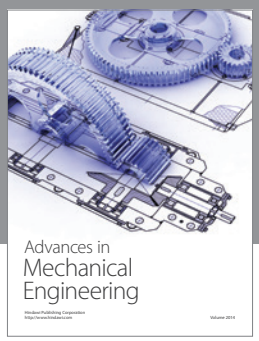

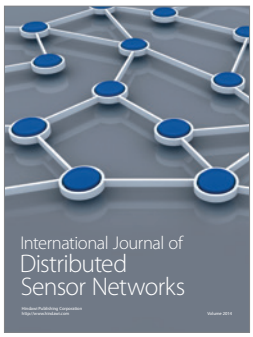

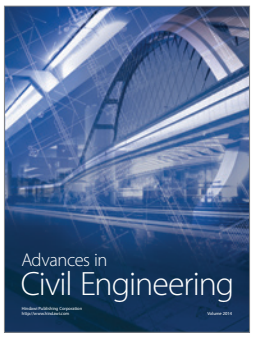

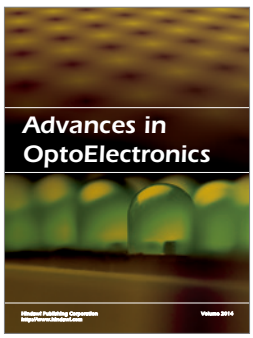

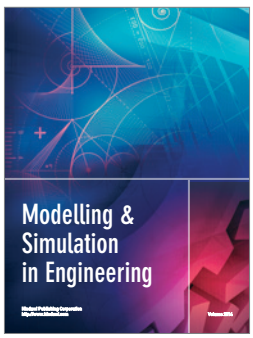

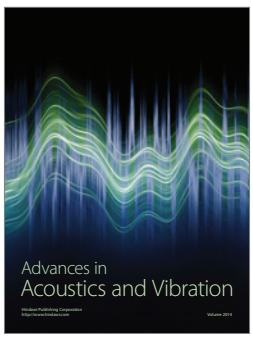

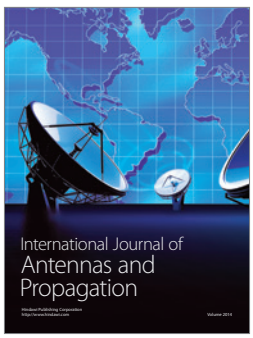

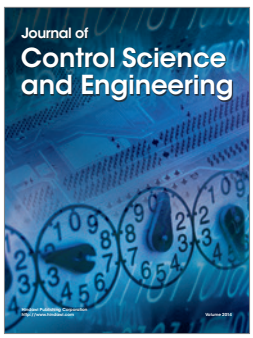

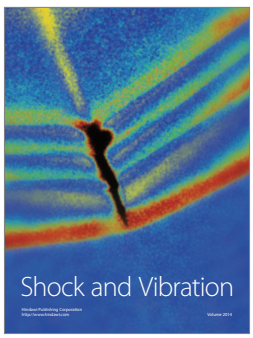

Hindawi

Submit your manuscripts at
http://www.hindawi.com